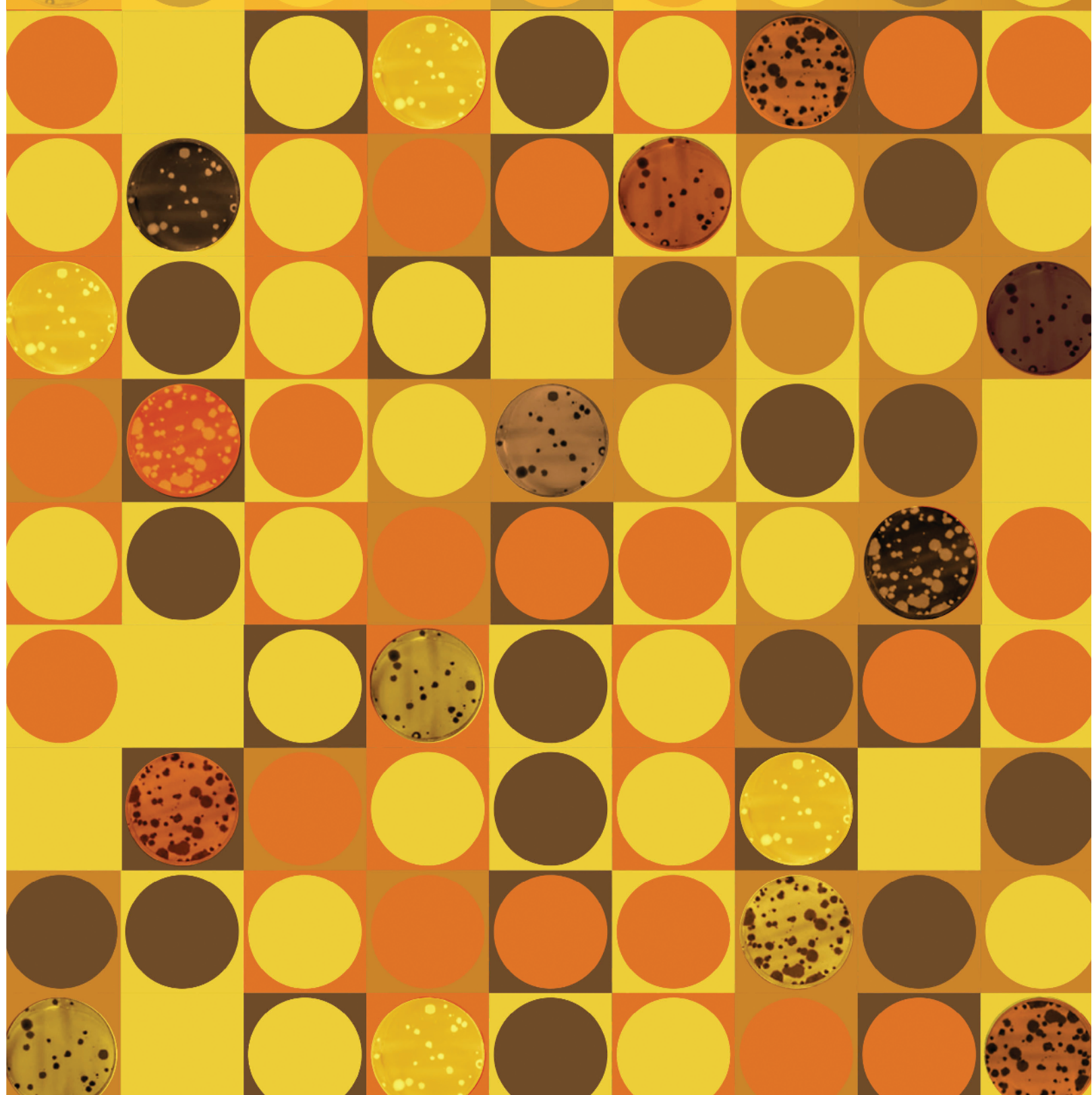


RESEARCH ARTICLE

# The p53 Target Gene SIVA Enables Non-Small Cell Lung Cancer Development

Jeanine L. Van Nostrand<sup>1</sup>, Alice Brisac<sup>2</sup>, Stephano S. Mello<sup>1</sup>, Suzanne B.R. Jacobs<sup>1</sup>, Richard Luong<sup>3</sup>, and Laura D. Attardi<sup>1,4</sup>



**ABSTRACT**

Although p53 transcriptional activation potential is critical for its ability to suppress cancer, the specific target genes involved in tumor suppression remain unclear. SIVA is a p53 target gene essential for p53-dependent apoptosis, although it can also promote proliferation through inhibition of p53 in some settings. Thus, the role of SIVA in tumorigenesis remains unclear. Here, we seek to define the contribution of SIVA to tumorigenesis by generating *Siva* conditional knockout mice. Surprisingly, we find that SIVA loss inhibits non-small cell lung cancer (NSCLC) development, suggesting that SIVA facilitates tumorigenesis. Similarly, SIVA knockdown in mouse and human NSCLC cell lines decreases proliferation and transformation. Consistent with this protumorigenic role for SIVA, high-level SIVA expression correlates with reduced NSCLC patient survival. SIVA acts independently of p53 and, instead, stimulates mTOR signaling and metabolism in NSCLC cells. Thus, SIVA enables tumorigenesis in a p53-independent manner, revealing a potential new cancer therapy target.

**SIGNIFICANCE:** These findings collectively reveal a novel role for the p53 target gene SIVA both in regulating metabolism and in enabling tumorigenesis, independently of p53. Importantly, these studies further identify SIVA as a new prognostic marker and as a potential target for NSCLC cancer therapy. *Cancer Discov*; 5(6): 622–35. © 2015 AACR.

See related commentary by Resnick-Silverman and Manfredi, p. 581.

**INTRODUCTION**

The p53 transcription factor is a critical tumor suppressor, as evidenced by the observations that it is mutated in over half of all human cancers and that *Trp53*-null mice develop cancer with 100% penetrance (1). p53 is a cellular stress sensor that triggers various cellular responses, including apoptosis, cell-cycle arrest, and autophagy (2, 3), in response to diverse stress signals, including DNA damage, hyperproliferative stimuli, and nutrient deprivation, as a measure to restrain tumorigenesis (1, 4). Although activation of apoptosis helps to eliminate defective cells, induction of cell-cycle arrest and the associated DNA repair program help to maintain the genetic integrity of cells and cell survival (2). p53 relies primarily on its function as a transcriptional activator to trigger these different responses through induction of a host of different target genes (1, 4). Although the specific target genes involved in cell-cycle arrest and apoptosis have been well characterized, the p53 target genes critical for tumor suppression remain incompletely understood (4, 5). Intriguingly, although transcriptional activation potential is critical for p53-mediated tumor suppression, canonical p53 target genes, such as *p21*

(*CDKN1A*), *PUMA* (*BBC3*), and *NOXA* (*PMAIP1*), are dispensable for tumor suppression (6–8). Thus, key mediators of p53 tumor-suppressor activity remain to be identified.

SIVA is a proapoptotic protein originally identified by virtue of its interaction with CD27 and other death receptors (9, 10). It was subsequently shown to be a direct p53 target gene that is specifically upregulated to high levels during apoptosis relative to G<sub>1</sub> cell-cycle arrest (11, 12). In addition, SIVA plays an important role in p53-dependent apoptosis *in vitro*, as loss of SIVA in cerebellar granular neurons (CGN) compromises DNA damage-induced, p53-dependent apoptosis (11). Furthermore, overexpression of SIVA in CGNs, mouse embryonic fibroblasts (MEF), and lymphocytes is sufficient to induce cell death (11, 13). In CGNs exposed to DNA damage, SIVA localizes to the plasma membrane and induces apoptosis in a manner dependent on BID and BAX/BAK (11), consistent with SIVA acting through both the extrinsic and intrinsic cell death pathways. This proapoptotic function suggests that SIVA may itself have tumor-suppressor activity.

Beyond its role in restraining cellular expansion through apoptosis, several lines of evidence suggest that SIVA also promotes proliferation. For example, *Siva* is directly transcriptionally activated by E2F1, a protein essential for promoting cell-cycle progression (12). In addition, SIVA has been reported to suppress p53 activity by stabilizing the interaction between MDM2 and p53, leading to increased p53 ubiquitination and degradation, and increased bromodeoxyuridine (BrdUrd) incorporation (14). SIVA can also act as an E3-ubiquitin ligase for the p53-activating protein p19<sup>ARF</sup>, thereby promoting p19<sup>ARF</sup> degradation, and consequently provoking p53 destabilization and enhanced cellular proliferation (15). Thus, these studies collectively suggest that SIVA could play a tumor-promoting role.

To explore whether SIVA exerts a tumor-suppressive or tumor-promoting role downstream of p53, we assessed the effect of SIVA loss in a mouse model of oncogenic KRAS-driven non-small cell lung cancer (NSCLC) development, in

<sup>1</sup>Division of Radiation and Cancer Biology, Department of Radiation Oncology, Stanford University School of Medicine, Stanford, California.

<sup>2</sup>Department of Biology, Ecole Normale Supérieure de Lyon, Lyon, France.

<sup>3</sup>Department of Comparative Medicine, Stanford University School of Medicine, Stanford, California. <sup>4</sup>Department of Genetics, Stanford University School of Medicine, Stanford, California.

**Note:** Supplementary data for this article are available at *Cancer Discovery* Online (<http://cancerdiscovery.aacrjournals.org/>).

**Corresponding Author:** Laura D. Attardi, Stanford University School of Medicine, 269 Campus Drive, CCSR-South, Room 1255, Stanford, CA 94305-5152. Phone: 650-725-8424; Fax: 650-723-7382; E-mail: attardi@stanford.edu

**doi:** 10.1158/2159-8290.CD-14-0921

© 2015 American Association for Cancer Research.

## RESEARCH ARTICLE

Van Nostrand et al.

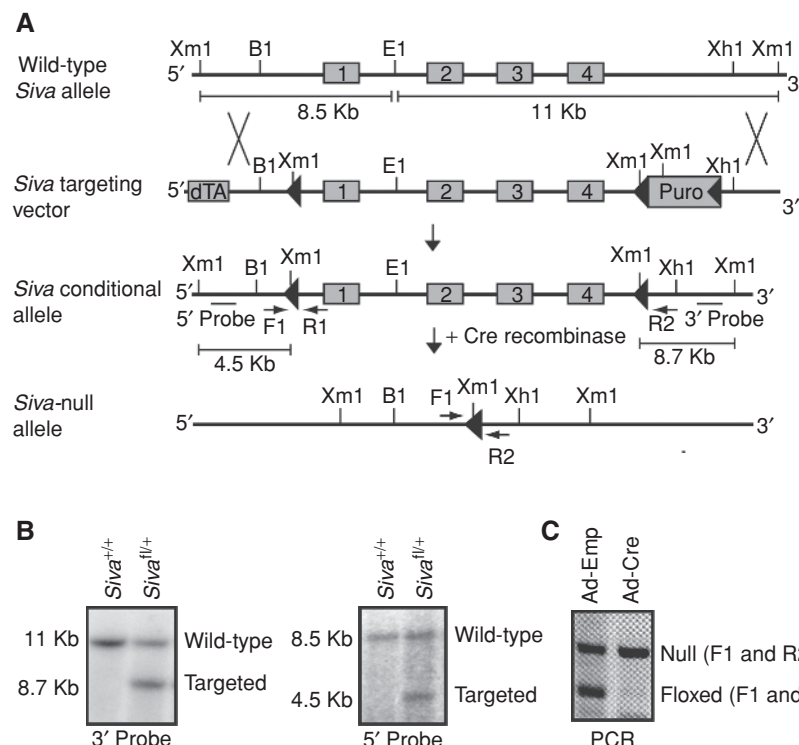


**Figure 1.** Generation of *Siva* conditional knockout mice. **A**, targeting scheme for generating *Siva* conditional knockout mice. The *Siva*-targeting vector contains a positive selection marker [Puromycin cassette (*Puro*)] flanked by *loxP* sites (triangles) and a negative selection marker [diphtheria toxin (dTA)]. The four exons comprising the *Siva* locus (gray boxes) are flanked by *loxP* and *Lox-Puro-Lox* sites on the 5' and 3' ends, respectively. The *Puro* cassette was removed *in vivo* by limited Cre expression, leaving a single 3' *loxP* site. Upon subsequent Cre recombinase expression, the *Siva* locus gets excised, resulting in a *Siva*-null allele. These recombination events were detected by Southern blot analysis using *Xmn1/EcoR1* restriction digests and subsequent probing with a 5' or 3' fragment external to the targeting vector. This leads to generation of fragments of different sizes in all cases, as shown. *B1*, *BamH1*; *E1*, *EcoR1*; *Xm1*, *Xmn1*; *Xh1*, *Xho1*. **B**, Southern blot analyses of mouse embryonic stem (ES) cells targeted at the *Siva* locus. Analyses of a wild-type (*Siva*<sup>+/+</sup>) and a targeted (*Siva*<sup>f/f</sup>) ES cell clone are shown. DNA was digested with *Xmn1/EcoR1*. Left, upon probing with the 3' probe, the 11-kb band indicates the wild-type allele and the 8.7-kb band indicates the targeted conditional allele. Right, upon probing with the 5' probe, the 8.5-kb band indicates the wild-type allele and the 4.5-kb band indicates the targeted conditional allele. **C**, PCR analysis of recombined allele. MEFs generated from E13.5 *Siva*<sup>f/f</sup> embryos (where f/f denotes the conditional knockout allele) were infected either with adenovirus-expressing Cre (Ad-Cre) to excise the floxed allele or with empty adenovirus (Ad-Emp) as a control. Primers spanning the 5' *loxP* site (F1 and R1) or the remaining *loxP* site after excision of the *Siva* locus (F1 and R2) were used. The absence of the floxed allele following Ad-Cre infection verifies the ability of Cre to fully excise the *Siva* locus.

which p53 plays a key role in suppressing malignant progression. Using *Siva* conditional knockout mice that we generated, we found that SIVA is necessary for efficient oncogenic KRAS-driven NSCLC development. Subsequent analysis of SIVA function *in vitro* revealed that SIVA knockdown dampens proliferation and transformation in both mouse and human NSCLC cell lines. The diminished proliferation and transformation upon SIVA knockdown are independent of p53 and, instead, are associated with decreased metabolic function. These findings indicate that SIVA plays a p53-independent role in enabling lung cancer development and suggest the possibility that it could ultimately be a target for cancer therapy.

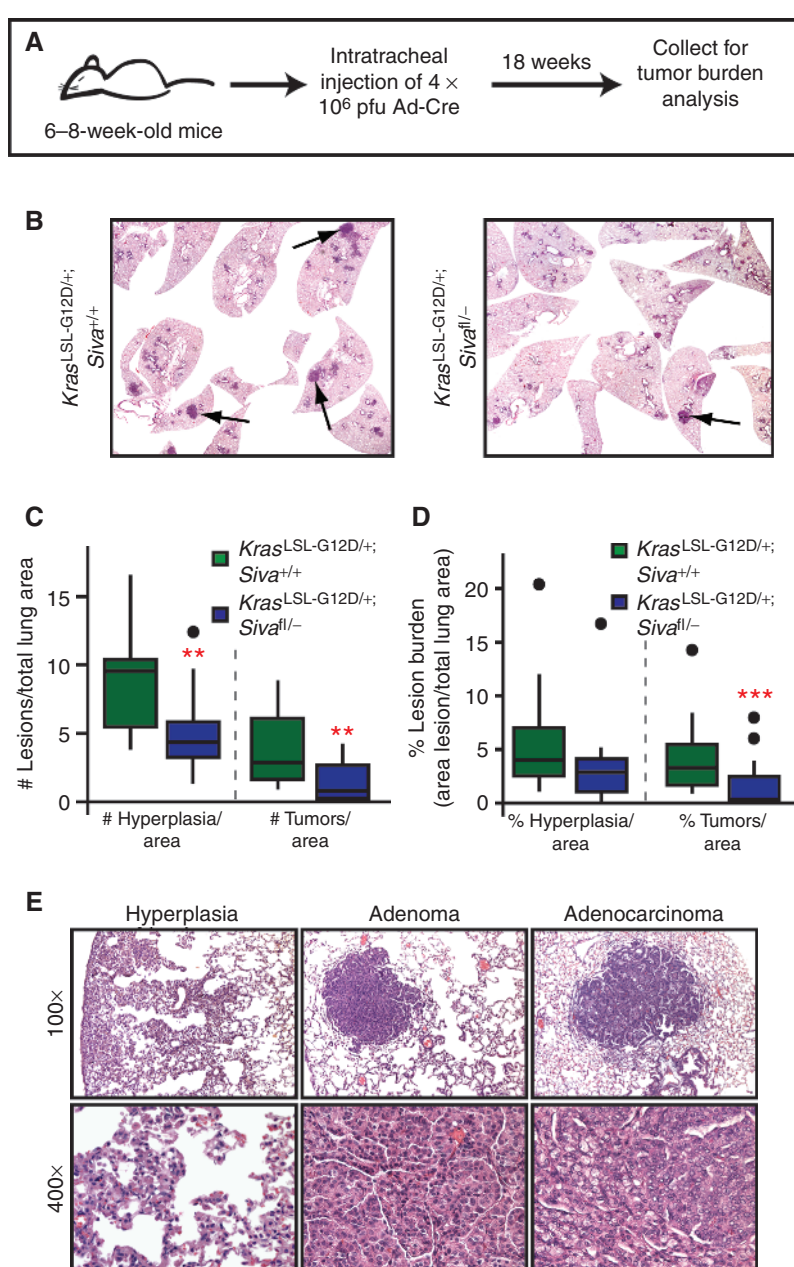
## RESULTS

Generation of *Siva* Conditional Knockout Mice

To analyze the role of SIVA in tumorigenesis *in vivo*, we generated *Siva* conditional knockout mice. Mouse embryonic stem (ES) cells were targeted such that the entire

*Siva* locus, comprising four exons, was flanked by a *loxP* and a *Lox-Puro-Lox* cassette, ensuring complete deletion of the *Siva* gene (Fig. 1A). Proper targeting of ES cells was confirmed by Southern blot analysis using both 5' and 3' external probes (Fig. 1B), and two independent lines of mice were generated. These mice were crossed to CMV-Cre transgenic mice (16), and progeny were screened for the presence of either a *Siva* conditional (denoted floxed or f/f) or *Siva*-null allele. To confirm that the floxed *Siva* allele could be efficiently recombined to generate *Siva*-null cells, MEFs derived from E13.5 *Siva*<sup>f/f</sup> embryos were infected with adenovirus-expressing Cre recombinase (Ad-Cre), and DNA was harvested. PCR verified that the floxed *Siva* allele was efficiently recombined, thereby producing *Siva*-null cells (Fig. 1C). Furthermore, analysis of progeny from crosses between mice heterozygous for the *Siva*-null allele revealed embryonic lethality of *Siva* homozygous mutant animals, similar to that observed previously with mice homozygous for a *Siva* gene-trapped allele (S.B.R. Jacobs and J.L. Van Nostrand, unpublished data; data not shown).

**Figure 2.** Siva deficiency inhibits lung tumorigenesis. **A**, schematic of the timeline for tumor study. Six- to 8-week-old mice were infected with Ad-Cre via intratracheal injection, and lungs were analyzed 18 weeks later. **B**, representative photomicrographs of lungs from *Kras*<sup>LSL-G12D</sup>; *Siva*<sup>+/+</sup> (left,  $n = 12$ ) and *Kras*<sup>LSL-G12D</sup>; *Siva*<sup>f/f</sup> (right,  $n = 17$ ) mice 18 weeks after Ad-Cre infection by intratracheal injection. **C**, box plot depicting the median number and quartiles of hyperplasias and tumors (adenomas and adenocarcinomas) per total lung area in *Kras*<sup>LSL-G12D</sup>; *Siva*<sup>+/+</sup> and *Kras*<sup>LSL-G12D</sup>; *Siva*<sup>f/f</sup> mice. Dots represent outlier data points. Hyperplasias: \*\*,  $P = 0.008$ ; tumors: \*\*,  $P = 0.0058$  by the Wilcoxon rank sum test between *Kras*<sup>LSL-G12D</sup>; *Siva*<sup>+/+</sup> and *Kras*<sup>LSL-G12D</sup>; *Siva*<sup>f/f</sup> mice. **D**, box plot depicting median tumor burden and quartiles calculated as tumor area per total lung area for hyperplasias and tumors (adenomas and adenocarcinomas). Dots represent outlier data points. Hyperplasia:  $P = 0.066$ ; tumors: \*\*\*,  $P = 0.003$  by Wilcoxon rank-sum test between *Kras*<sup>LSL-G12D</sup>; *Siva*<sup>+/+</sup> and *Kras*<sup>LSL-G12D</sup>; *Siva*<sup>f/f</sup> mice. **E**, representative photomicrographs of hyperplasias and tumors (adenomas and adenocarcinomas) taken at  $\times 100$  and  $\times 400$  magnification.



### SIVA Enables KRAS-Induced Lung Tumorigenesis

To determine the role of SIVA in tumorigenesis, we chose an NSCLC model in which p53 has been shown to play a critical role in suppressing tumor progression (17). In this model, activated KRAS<sup>G12D</sup> drives the development of lung adenomas, which progress to adenocarcinomas in the absence of p53 (5, 17). We used *Kras*<sup>LSL-G12D</sup> mice, in which an upstream floxed transcriptional stop cassette (*Lox-Stop-Lox*) silences KRAS<sup>G12D</sup> expression until Cre recombinase is introduced. We generated cohorts of *Kras*<sup>LSL-G12D</sup>; *Siva*<sup>+/+</sup>, *Kras*<sup>LSL-G12D</sup>; *Siva*<sup>f/f</sup>, *Kras*<sup>LSL-G12D</sup>; *Siva*<sup>+/−</sup>, and *Kras*<sup>LSL-G12D</sup>; *Siva*<sup>−/−</sup> mice, which we infected with Ad-Cre through intratracheal injection (18) to drive expression of KRAS<sup>G12D</sup> and excision of the *Siva* locus. Mice were subjected 18 weeks later to a

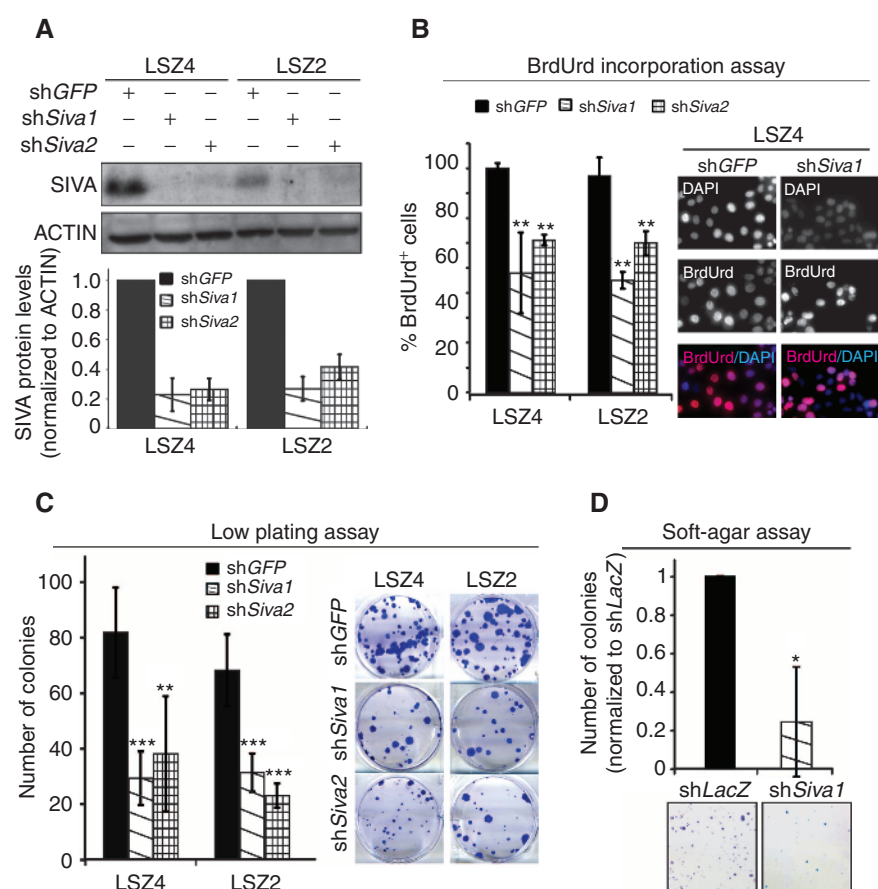
quantitative analysis of tumor development (Fig. 2A). Surprisingly, histologic analyses revealed fewer tumors, including both adenomas and adenocarcinomas, and reduced tumor burden (percentage of lung area comprising tumors) in *Kras*<sup>LSL-G12D</sup>; *Siva*<sup>f/f</sup> mice compared with *Kras*<sup>LSL-G12D</sup>; *Siva*<sup>+/+</sup> control mice. *Kras*<sup>LSL-G12D</sup>; *Siva*<sup>f/f</sup> mice also had reduced burden of hyperplastic lesions compared with controls (Fig. 2B–E). In addition, we observed reduced tumor number and tumor burden in *Siva* heterozygous mice (*Kras*<sup>LSL-G12D</sup>; *Siva*<sup>f/f</sup>, *Kras*<sup>LSL-G12D</sup>; *Siva*<sup>+/−</sup>) relative to *Kras*<sup>LSL-G12D</sup>; *Siva*<sup>+/+</sup> controls (Supplementary Fig. S1A and S1B). Furthermore, the tumor burden and tumor number in *Kras*<sup>LSL-G12D</sup>; *Siva*<sup>−/−</sup> mice were comparable with those observed in *Kras*<sup>LSL-G12D</sup>; *Siva*<sup>f/f</sup> mice. Together, these observations indicate that SIVA loss impedes tumor initiation, and that SIVA normally enables tumorigenesis.

## RESEARCH ARTICLE

Van Nostrand et al.

## Siva Knockdown Inhibits Mouse NSCLC Cell Proliferation

To explore the mechanisms underlying the decreased tumorigenesis observed following SIVA inactivation, we used two mouse NSCLC cell lines, LSZ2 and LSZ4, generated previously by serial allograft passage of tumors derived from *Kras*<sup>G12D</sup>;Trp53<sup>+/-</sup> mice. Importantly, these tumor cells still harbor wild-type p53 (19) and express SIVA (Fig. 3A). We used two independent shRNAs directed against *Siva* and achieved a 70% to 80% reduction in SIVA protein levels following lentiviral transduction with each (Fig. 3A). We first analyzed the proliferative capacity of cells upon *Siva* knockdown by assessing BrdUrd incorporation. Perturbation with either *Siva* shRNA resulted in a significant decrease in the percentage of BrdUrd-positive cells in both cell lines relative to control GFP shRNA (Fig. 3B), indicating that SIVA facilitates proliferation. In contrast, depleting SIVA by infecting *Siva*<sup>fl/fl</sup> MEFs with Ad-Cre or knocking down *Siva* in pancreatic cancer cell lines did not affect the proliferative index (Supplementary Fig. S2A and S2B), suggesting that SIVA's role in facilitating proliferation is cell type specific or context specific. Notably, *Siva* knockdown in LSZ4 cells did not augment the percentage of Annexin V-positive cells, indicating that increased apoptosis is not responsible for diminished tumor burden (Supplementary Fig. S3A and S3B). Next, to more directly explore whether *Siva* knockdown affects the transformation properties of NSCLC cells, we assessed the ability of cells to form colonies upon low-density plating and upon anchorage-independent growth in soft agar.



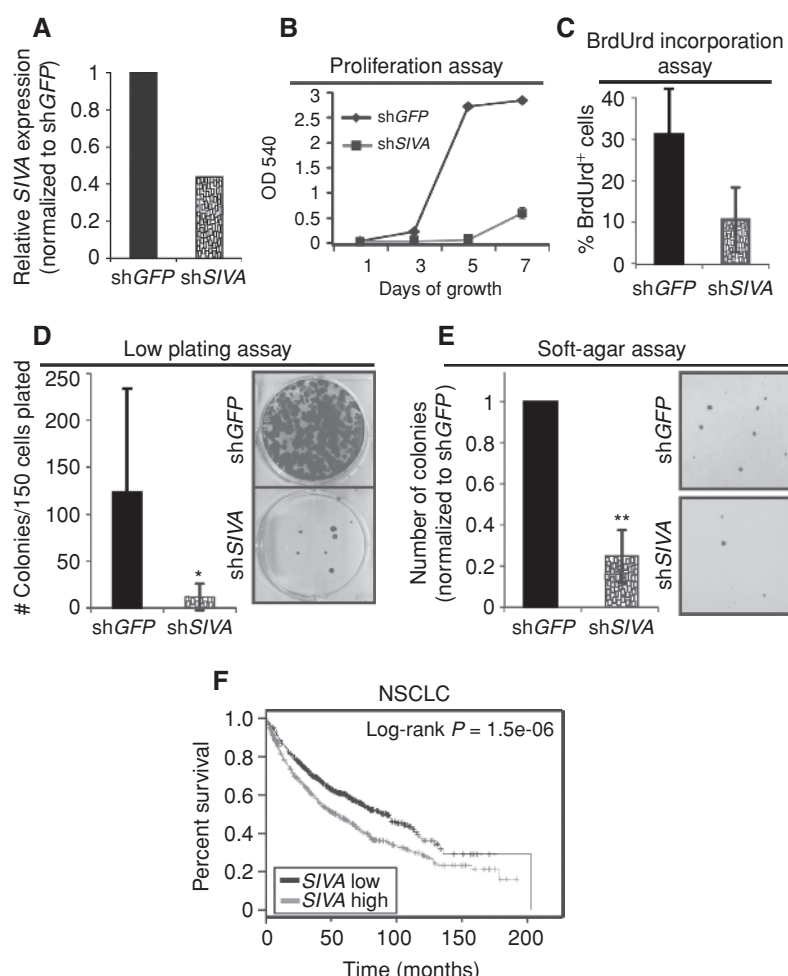
*Siva* knockdown resulted in fewer colonies forming in the low-density plating assay compared with shGFP control-expressing cells (Fig. 3C). Similarly, using a soft-agar assay, fewer colonies were able to form upon *Siva* knockdown than with shLacZ control shRNA (Fig. 3D). Together, these results suggest that SIVA enhances proliferation and transformation, thus recapitulating our findings in the *in vivo* tumorigenesis study.

## SIVA Knockdown Inhibits Human NSCLC Cell Proliferation

To determine whether the role for SIVA in promoting efficient tumorigenesis in mouse cells is conserved in human cells, we next examined whether SIVA similarly facilitates the proliferation of human A549 NSCLC cells expressing oncogenic KRAS<sup>G12S</sup> and wild-type p53. We knocked down SIVA in A549 cells using lentiviral transduction of SIVA shRNAs and observed depletion of SIVA mRNA by quantitative RT-PCR (Fig. 4A). We assessed the importance of SIVA for cellular proliferation by generating growth curves and measuring BrdUrd incorporation. As observed in the mouse LSZ4 and LSZ2 cell lines, SIVA knockdown in A549 cells results in reduced proliferative potential relative to the shGFP control (Fig. 4B and C). Furthermore, knockdown of SIVA inhibited colony formation in both low-density plating and soft-agar assays relative to the shGFP control, revealing an important role for SIVA in promoting transformation (Fig. 4D and E). These results demonstrate that SIVA enhances proliferation and transformation not only in mouse NSCLC cells but also in human

**Figure 3.** *Siva* knockdown inhibits cellular proliferation and transformation in mouse NSCLC cells. **A**, top, Western blot analysis of SIVA in LSZ4 and LSZ2 NSCLC cell lines. Two independent shRNAs targeting *Siva* were used to knock down *Siva*. shRNA targeting GFP was used as a negative control. ACTIN serves as a loading control. Bottom, quantification of SIVA protein levels following expression of two *Siva* shRNAs compared with expression of shGFP, after normalization to ACTIN. **B**, left, average percentage of BrdUrd incorporation upon *Siva* knockdown in LSZ4 and LSZ2 cells compared with control knockdown with shGFP. Error bars,  $\pm$ SD. *P* values by the Student *t* test comparing each shRNA to shGFP: LSZ4: \*\*, *P* = 0.006, 0.002; LSZ2: \*\*, *P* = 0.003, 0.007. Right, representative images of BrdUrd immunofluorescence. Blue, DAPI; red, BrdUrd. **C**, Left, average number of colonies in low plating assay upon *Siva* knockdown in LSZ4 and LSZ2 cells compared with control knockdown with shGFP. Error bars,  $\pm$ SD. *P* values by the Student *t* test: LSZ4: \*\*\*, *P* = 0.0002; \*\*, *P* = 0.0025; LSZ2: \*\*\*, *P* = 0.0004, 0.0001. Right, representative images of colonies in low plating assay stained with crystal violet. **D**, Top, average number of colonies in soft-agar assay upon *Siva* knockdown in LSZ4 cells relative to control knockdown with shLacZ. Error bars,  $\pm$ SD. \*, *P* value by the Student *t* test: 0.047. Bottom, representative images of colonies in soft-agar assay stained with Giemsa. DAPI, 4,6-diamidino-2-phenylindole.

**Figure 4.** SIVA knockdown inhibits cellular proliferation and transformation in human NSCLC cells. **A**, SIVA expression in A549 cells, as assessed by quantitative RT-PCR normalized to  $\beta$ -Actin, upon expression of shRNA targeting SIVA or shRNA targeting GFP. **B**, representative cellular proliferation assay in A549 cells over 7 days following SIVA or control GFP shRNA transduction. The experiment was repeated in duplicate with two independent shRNAs to SIVA each time. **C**, average percentage of BrdUrd incorporation in SIVA knockdown cells. Error bars,  $\pm$ SD. P value by the Student t test: 0.058. **D**, left, average number of colonies in low plating assay following SIVA or control GFP shRNA transduction. Error bars,  $\pm$ SD. Right, representative images of colonies in low plating assay stained with crystal violet. \*, P value by the Student t test: 0.05. **E**, left, average number of colonies in soft-agar assay upon knockdown of SIVA relative to control cells expressing shGFP. Error bars,  $\pm$ SD. \*\*, P value by the Student t test: 0.0013. Right, representative images of soft-agar assay stained with Giemsa. **F**, survival curve from human NSCLC patients generated using KMplot.com and gene expression from the SIVA1 probe 203489\_at. SIVA expression levels: low, black; high, gray.



NSCLC cells. Supporting the idea that SIVA expression can promote tumorigenesis, analysis of survival data for human NSCLC patients revealed that patients with lung cancers expressing high levels of SIVA have significantly reduced overall survival than those with lung cancers expressing low levels of SIVA (Fig. 4F; refs. 20, 21). Thus, SIVA expression levels have prognostic power in human NSCLC patients.

#### Siva Knockdown Inhibits Proliferation and Transformation in a p53-Independent Manner

Decreased proliferative capacity and suppression of transformation ability are well-known effects of p53 activation. It has previously been reported that SIVA can negatively regulate p53 by stabilizing the p53-MDM2 interaction and by promoting p19<sup>ARF</sup> degradation and that SIVA loss can therefore induce p53 activity (14, 15). We therefore sought to test whether stabilization and activation of p53 provokes the inhibition of proliferation and transformation we observed upon SIVA inactivation in NSCLC cells. First, we assessed p53 protein levels and activity upon *Siva* knockdown in LSZ4 cells. Western blot analysis of p53 in LSZ4 cells after *Siva* knockdown revealed no difference in p53 levels, despite a clear inhibition of proliferation (Fig. 5A). Second, because p53 is a transcriptional activator, we analyzed p53 target gene expression as a readout of p53 activity. Upon *Siva* knockdown

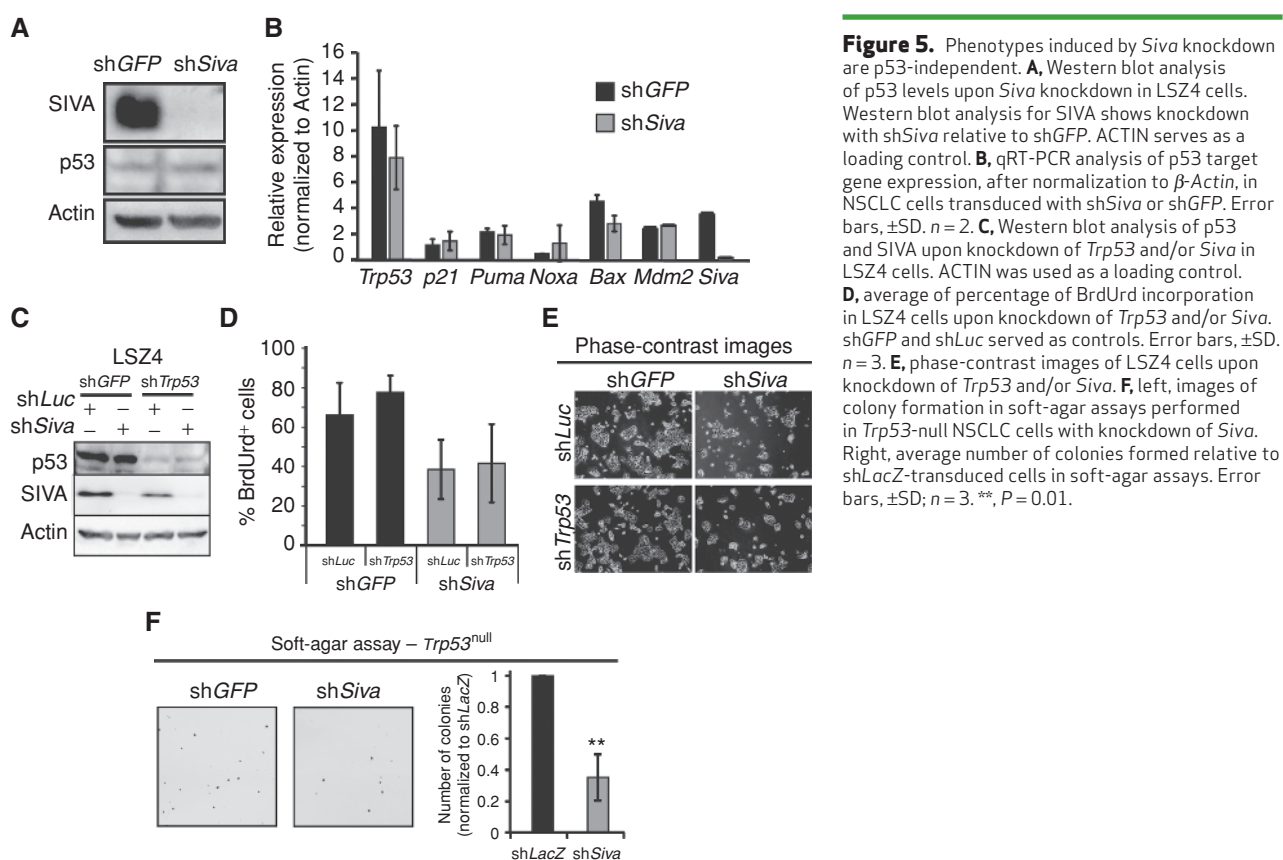
in LSZ4 cells, we observed no difference in p53 target gene expression relative to shGFP-expressing cells, suggesting that SIVA does not stimulate proliferation in NSCLC cell lines by inactivating p53, as previously described (Fig. 5B). Finally, we investigated whether p53 is required for the phenotypic effects of *Siva* knockdown. Upon attenuation of both *Trp53* and *Siva* in LSZ4 cells using RNA interference, we assessed BrdUrd incorporation and found that additional knockdown of *Trp53* does not rescue the inhibition of proliferation triggered by SIVA loss (Fig. 5C–E). These results were bolstered by analysis of *Trp53*-null NSCLC cell lines, where we observed that *Siva* knockdown also causes decreased transformation in soft-agar assays, similarly to *Siva* knockdown in p53-expressing LSZ4 cells (Fig. 5F). Thus, the inhibition of proliferation caused by attenuated *Siva* expression does not rely on p53.

#### Siva Knockdown Alters Expression of Metabolic Genes

To gain an understanding of the molecular basis for the reduced proliferation and transformation resulting from *Siva* knockdown, we performed gene expression profiling experiments on LSZ4 and LSZ2 cells after *Siva* knockdown by lentiviral transduction with each of the two previously characterized shRNAs (*shSiva1* and *shSiva2*) and each of two control shRNAs (*shLacZ* and *shGFP*). Hierarchical clustering revealed a notable

## RESEARCH ARTICLE

Van Nostrand et al.



difference in gene expression profiles between *Siva* knockdown and control samples (Fig. 6A). Differentially expressed genes were analyzed for enrichment in Gene Ontology (GO) terms using GeneSpring Analysis. We found that the most enriched GO terms included immune regulation—consistent with SIVA's known role in regulating NF-κB signaling—as well as cell migration and metabolic processes (Fig. 6B). We first queried whether altered NF-κB signaling could be responsible for the decreased proliferation upon SIVA loss by Western blot analysis of activated p65, a component of canonical NF-κB (22) signaling. However, neither p65 nor phospho-p65 levels were altered upon *Siva* knockdown in LSZ4 cells (Supplementary Fig. S4A). Moreover, although SIVA has been shown to impinge upon NF-κB signaling through inhibition of the TGFβ activated kinase 1 (TAK1; ref. 23), we found that pharmacologic TAK1 inhibition (22) was not able to rescue the reduced proliferation caused by *Siva* knockdown (Supplementary Fig. S4B). These findings suggest that the known role of SIVA in NF-κB signaling does not account for the protumorigenic effects of SIVA. Thus, given the critical role for the appropriate regulation of metabolism in cancer cell proliferation and survival, we next sought to investigate a potential role for SIVA in regulating metabolism.

### Siva Knockdown Decreases Metabolic Activity and Induces Autophagy

To interrogate the role of SIVA in regulating metabolism, we first examined whether metabolic function is altered upon *Siva* knockdown by measuring oxygen consumption rates

(OCR) and extracellular acidification rates (ECAR), as indicators of oxidative phosphorylation and glycolytic rates, respectively. These analyses revealed that knockdown of *Siva* in both LSZ4 and LSZ2 cells decreases mitochondrial respiration and, less dramatically, glycolysis, suggesting an overall reduction in metabolic function (Fig. 6C and data not shown). Specifically, although the basal oxidative phosphorylation rate was reduced slightly upon *Siva* knockdown, the maximal mitochondrial respiration capacity, measured upon treatment with the ATP synthesis-electron transport uncoupler FCCP, was significantly decreased upon *Siva* knockdown. Treatment with either oligomycin, an ATP synthase inhibitor that reveals the OCR associated with mitochondrial proton leak, or antimycin, a mitochondrial complex III inhibitor that disrupts the proton gradient and reveals mitochondrial-independent oxygen consumption, did not cause any significant change in OCR upon SIVA inhibition, suggesting a specific role for SIVA in mitochondrial metabolism. To investigate why mitochondrial function is decreased upon *Siva* knockdown, we examined mitochondrial content by quantifying mitochondrial DNA, specifically the mitochondrial *Cox3*, *CytB*, and *16S rRNA* genes. Quantitative PCR revealed that mitochondrial DNA content is reduced by approximately 40% in both LSZ2 and LSZ4 cells upon *Siva* knockdown, providing a basis for the decreased mitochondrial respiration function (Fig. 6D). These results suggest that SIVA is critical for promoting efficient metabolism through the mitochondria, and thus SIVA may normally promote proliferation by facilitating efficacious ATP production.

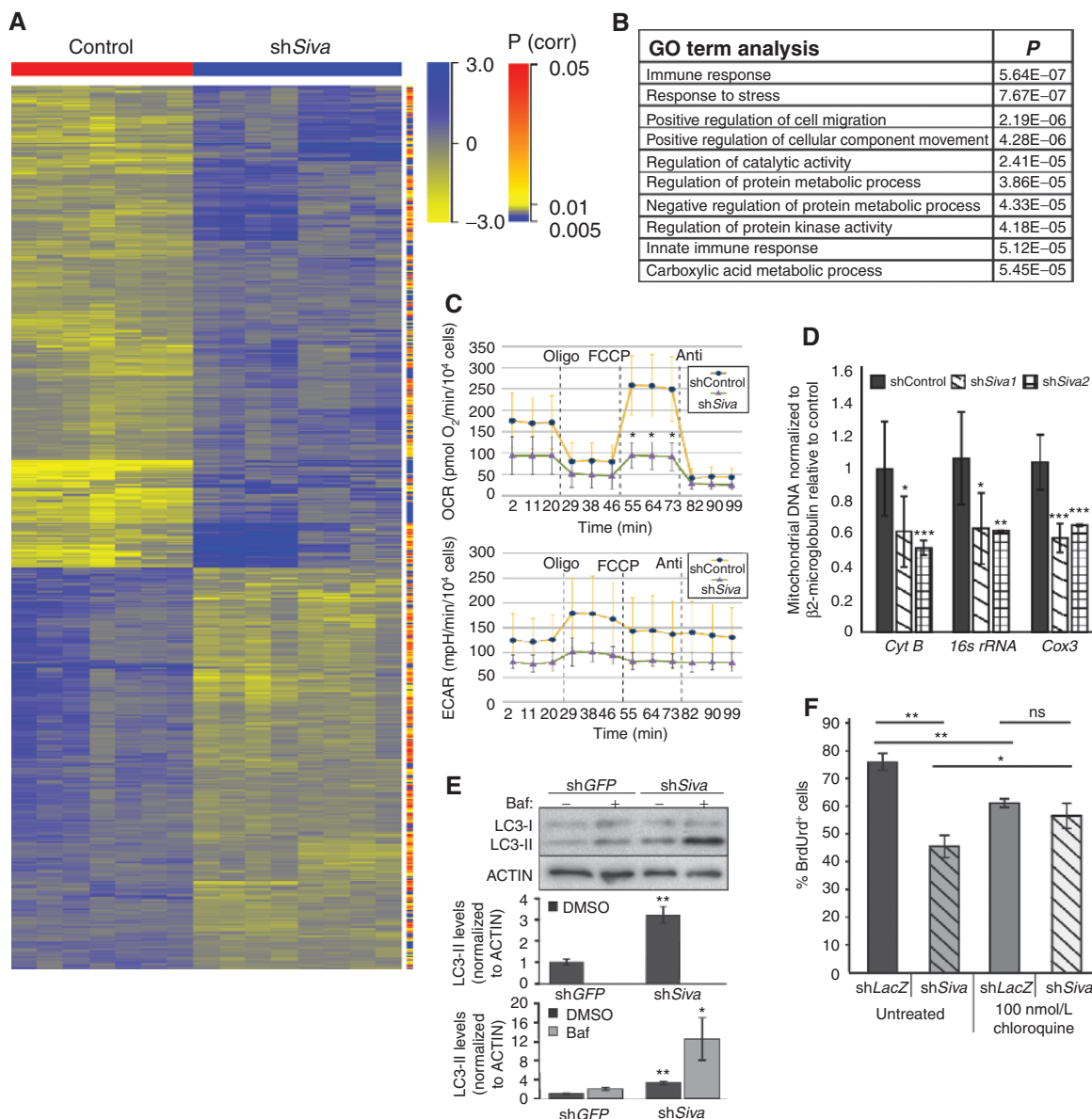


**Figure 6.** SIVA loss decreases metabolic function of NSCLC cells. **A**, heatmap of gene expression based on hierarchical clustering of microarray data from LSZ2 and LSZ4 cells with control knockdown using two control hairpins (shGFP and shLacZ; red) or knockdown of Siva using two independent hairpins (shSiva1 and shSiva2; blue). Genes identified for the heatmap were significantly modulated (*P* value less than or equal to 0.05) and had a fold change equal to or greater than 1.5. Yellow signifies downregulated genes, and blue signifies upregulated genes. *P* value for each gene is denoted on the right-hand side with either red (high) or blue (low) bars. **B**, GO term analysis of genes with altered expression upon Siva shRNA transduction into LSZ2 and LSZ4 cells relative to cells with control shRNA transduction. The *P* value for each category is shown on the right side. GO term analysis was performed using GeneSpring-GX software (Agilent). **C**, OCR and ECAR in LSZ4 cells upon Siva knockdown or in shGFP-transduced control cells. Oligo, oligomycin [ATP synthase inhibitor (electron transport chain inhibitor)]; FCCP (uncoupler); anti, antimycin (proton gradient disrupter). \*, *P* value by the Student *t* test: 0.024. **D**, mitochondrial DNA content assessed by quantitative PCR for mitochondrial-encoded genes upon knockdown of Siva in LSZ4 cells and in shGFP-transduced control cells. Normalized to β2-microglobulin. \*, *P* < 0.05; \*\*, *P* < 0.01; \*\*\*, *P* < 0.005. **E**, top, Western blot analysis of autophagy related protein LC3-II in LSZ4 cells upon shSiva or shGFP control transduction. ACTIN used as a loading control. Bottom, quantification of LC3-II levels upon Siva knockdown without (top) and with Bafilomycin A1 (Baf; bottom), relative to ACTIN. *P* value by the Student *t* test: \*, 0.05; \*\*, 0.007. **F**, average percentage of BrdUrd incorporation in LSZ4 cells with control (shLacZ) or Siva (shSiva) knockdown in the absence (untreated) or presence of chloroquine. Cells were incubated with 100 nmol/L chloroquine for 18 hours prior to BrdUrd pulse. Graph represents average ± SD of three experiments. \*, *P* < 0.05; \*\*, *P* < 0.01; ns, not significant by the Student *t* test. *n* = 3.

An important homeostatic response of cells to decreased energy production is to induce autophagy, a process by which organelles and cytoplasmic proteins are degraded for either energy production or quality control. We therefore sought to query whether autophagy might be induced upon Siva knockdown. We assessed levels of autophagy by immunoblotting

for modified LC3 (LC3-II), which is generated from LC3-I upon conjugation of phosphatidylethanolamine and then incorporated into autophagic vesicles, thus serving as a marker of autophagy. To confirm that any enhanced LC3-II signal represents increased autophagic flux, rather than a block in autophagy resulting in the accumulation of

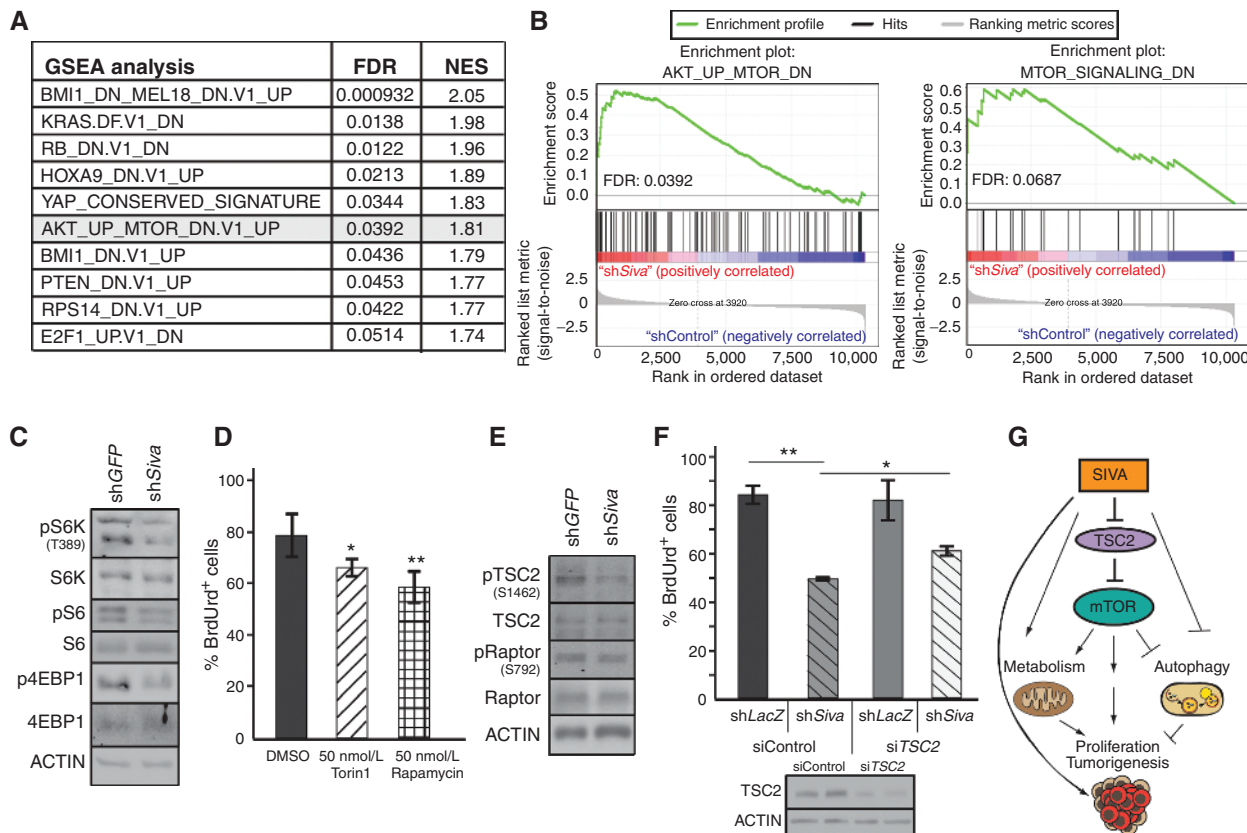


**Figure 7.** SIVA loss decreases metabolic function of NSCLC cells. **A**, gene set enrichment analysis (GSEA) of genes with altered expression upon *Siva* shRNA transduction into LSZ2 and LSZ4 cells relative to cells with control shRNA transduction. The FDR P value and normalized enrichment score (NES) for each category are shown on the right side. The GSEA signature for decreased mTOR signaling is highlighted in gray. **B**, select GSEA profiles (left) enrichment of genes upregulated upon mTOR inhibition in the presence of AKT upregulation. FDR q-value: 0.039 (right) enrichment of genes downregulated upon mTOR activation. FDR q-value: 0.069. **C**, Western blot analysis of mTOR signaling targets in LSZ4 cells upon shSiva or shGFP control transduction. ACTIN serves as a loading control. **D**, average percentage of BrdUrd incorporation in LSZ4 cells treated with 50 nmol/L Torin1 or 50 nmol/L rapamycin for 18 hours. Error bars,  $\pm$ SD. P value by the Student t test: \*, Torin1: 0.048; \*\*, rapamycin 0.009. **E**, Western blot analysis of mTOR upstream signaling components in LSZ4 cells upon shSiva or shGFP control transduction. ACTIN serves as a loading control. **F**, average percentage of BrdUrd incorporation in LSZ4 cells with control (shLacZ) or *Siva* (shSiva) knockdown and without (siControl) or with TSC2 (siTsc2) knockdown. Error bars,  $\pm$ SD; \*,  $P < 0.05$ ; \*\*,  $P < 0.01$  by the Student t test. **G**, model depicting the role of SIVA in promoting tumorigenesis through activation of mTOR signaling, which can itself affect metabolism, proliferation, tumorigenesis, and autophagy. SIVA may also have mTOR-independent effects on these processes.

autophagosomes, we also analyzed cells treated with Bafilomycin A1 (Baf), an inhibitor of autophagic vesicle maturation. We observed an increase in LC3-II levels upon *Siva* knockdown relative to the shGFP control, which was further enhanced with Baf treatment, indicating that SIVA inhibition triggers increased autophagic flux (Fig. 6E). To determine whether the increased autophagy associated with *Siva* knockdown could be responsible for decreasing proliferation, as occurs with AMBRA1 or UVRAg overexpression (24, 25), we inhibited autophagy using chloroquine and analyzed BrdUrd incorporation in *Siva* knockdown cells. Inhibition of autophagy was indeed able to partially rescue the dampened proliferation upon *Siva* knockdown (Fig. 6F), suggesting that the increased autophagy contributes to the reduced proliferation and tumorigenic potential upon *Siva* loss. We also observed that inhibition of autophagy decreased proliferation in control cells, suggesting that efficient proliferation relies on some level of autophagy. These observations collectively suggest that SIVA normally suppresses autophagy,

possibly either indirectly by maintaining proper energy production or directly by negatively regulating an upstream signaling pathway triggering autophagy.

### SIVA Enhances mTOR Activity

To gain insight into the molecular underpinnings of SIVA function in metabolism and autophagy, we examined signaling pathways through which SIVA might act. We first analyzed the genes modulated upon *Siva* knockdown using gene set enrichment analysis (GSEA) and found an enrichment for signatures associated with decreased proliferation, occurring with diminished KRAS, E2F1, and mTOR signaling or increased RB activity (Fig. 7A). We also identified signatures associated with increased NF- $\kappa$ B signaling (TBK1 activation; KRAS.DF.V1\_DN; ref. 26), decreased ribosomal function (RPS14\_DN.V1\_UP), and decreased chromatin remodeling activity/histone modification (BMI1\_DN.V1\_UP). We found mTOR signaling to be a particularly compelling pathway to pursue given the numerous parallels seen between SIVA and

mTOR, which also has a known role in regulating mitochondrial metabolism, inhibiting autophagy, promoting cell proliferation, and supporting tumorigenesis (27). These observations, coupled with our finding that *Siva* knockdown produces a signature resembling those associated with decreased mTOR signaling, suggest that SIVA may promote mTOR signaling (Fig. 7B). To test this hypothesis, we first examined whether *Siva* knockdown results in decreased mTOR activity by analyzing phosphorylation of the mTOR substrates S6 kinase (S6K) and 4EBP1 as well as the S6K substrate S6. Indeed, we observed a reduction in phospho-S6K, phospho-S6, and phospho-4EBP1 levels upon *Siva* knockdown, indicative of diminished mTOR activity, consistent with the gene expression data (Fig. 7C). These findings indicate that SIVA is indeed necessary for full mTOR activity. We next examined whether reduced mTOR activity results in diminished proliferation in LSZ4 cells. We used two mTOR inhibitors, Torin1 and rapamycin, which target mTOR complex 1 and both mTOR complexes 1 and 2, respectively, and quantified the rate of BrdUrd incorporation. Similar to *Siva* knockdown, inhibition of mTOR activity significantly decreased the proliferation of LSZ4 cells, suggesting that mTOR activity is indeed necessary for maximal LSZ4 cell proliferation (Fig. 7D).

mTOR is regulated either by AMPK, which inhibits mTOR activity through phosphorylation and inhibition of RAPTOR at S722/S792 and phosphorylation and activation of TSC2 at S1387, or by mitogenic signaling pathways, which activate mTOR by phosphorylating and inhibiting TSC2 at S1462 (27). To determine how SIVA inhibits mTOR activity, we examined the phosphorylation of RAPTOR at S792, as a marker of AMPK signaling, and phosphorylation of TSC2 at S1462, as a marker of mitogenic signaling pathways. Although we observed no difference in phospho-RAPTOR levels in cells with different *Siva* status, we observed a decrease in phospho-S1462 TSC2 levels upon *Siva* knockdown, suggesting that SIVA acts through mitogenic signaling rather than AMPK signaling to promote mTOR activity (Fig. 7E). Together, these findings reveal that SIVA is essential for maximal mTOR activity, which is necessary for optimal proliferation in LSZ4 cells.

To determine whether decreased mTOR activity is responsible for the proliferation defects upon *Siva* knockdown, we tested whether reactivation of mTOR signaling through knockdown of *Tsc2* could rescue BrdUrd incorporation in sh*Siva*-transduced cells. Indeed, with approximately 50% knockdown of *Tsc2*, we observed a partial rescue in BrdUrd incorporation in sh*Siva*-transduced cells and no effect in control cells (Fig. 7F). Collectively, these findings reveal a novel role for SIVA in promoting mTOR activity and metabolism, which is necessary for enhancing proliferation and tumorigenesis downstream of oncogenic KRAS (Fig. 7G).

## DISCUSSION

Here, we describe a critical role for the p53 target gene SIVA in facilitating NSCLC development. Conditional inactivation of *Siva* in an autochthonous oncogenic KRAS<sup>G12D</sup>-driven model for NSCLC resulted in decreased tumor numbers and tumor burden relative to SIVA-expressing controls. More-

over, we found that SIVA knockdown inhibits proliferation and transformation in both mouse and human NSCLC cells *in vitro*. We discovered further that SIVA does not exert its protumorigenic effect by restraining p53. Instead, the enhancement of tumorigenesis by SIVA relates to its ability to promote mTOR signaling, inhibit autophagy, and augment metabolic activity (28–30). Consistent with this protumorigenic role, high-level SIVA expression correlates with worse prognosis in NSCLC patients (20).

Previous reports showed that SIVA loss promotes p53 stabilization and inhibits proliferation, attributable to SIVA function in enabling p53-MDM2 interactions and in enhancing ubiquitin-mediated p19<sup>ARF</sup> degradation (14, 15). In contrast, we found that p53 activation is not responsible for the inhibition of proliferation upon SIVA loss, as p53 was not induced upon *Siva* attenuation and *Siva* knockdown could inhibit proliferation and transformation irrespective of p53 status. However, the observation that SIVA is able to promote tumorigenesis reveals an intriguing contradiction with respect to its role as a p53 target gene, perhaps reflecting the fact that p53 target genes are often regulated by additional transcription factors and function in a p53-independent manner in some contexts. For example, SIVA can also be induced by the E2F1 transcription factor, which can play both tumor-suppressive and oncogenic roles (12, 31). Such a protumorigenic role of a p53 target gene recalls *TIGAR*, a p53 target gene involved in cell survival upon oxidative stress, which promotes tumorigenesis in a mouse small-intestinal cancer model (32). Moreover, *TIGAR* is thought to be upregulated in a p53-independent manner in human tumors (33). Our work similarly suggests that SIVA plays a p53-independent role in promoting proliferation and tumorigenesis.

Although SIVA clearly alters the metabolic capacity of NSCLC cells, reflected by enhanced mitochondrial respiration and reduced autophagy, it remains unclear precisely how SIVA exerts these effects. SIVA may affect metabolism by stimulating mTOR signaling, which is known to enhance oxidative metabolism, at least in part, via activation of S6K and 4EBP1 and consequent translation of nuclear-encoded mitochondrial proteins (34, 35), and to dampen autophagy through phosphorylation and inactivation of the autophagy-initiating kinase ULK1/ATG1 (36). Moreover, mTOR is known to promote tumorigenesis in mouse hepatocellular, renal, and lung cancer models (28, 29, 37, 38). Thus, a role for SIVA in the positive regulation of mTOR could account for the decreased oxidative phosphorylation, increased autophagy, and reduced tumor burden with SIVA deficiency (27, 34, 36, 38). Based on our Western blot analyses of upstream signaling pathway components, SIVA appears to exert effects on mTOR signaling not through the negative regulator AMPK, which responds to cellular energy levels, but rather through positively regulating mitogenic signaling pathways, such as the ERK1/2, WNT, and AKT signaling pathways, which respond to growth signals (27, 37). However, the exact mechanisms by which SIVA activates these mitogenic signaling pathways and which mitogenic signaling pathways are most important remain to be elucidated.

An alternative mechanism for SIVA action is that it affects metabolism through pathways related to its apoptotic function.

## RESEARCH ARTICLE

Van Nostrand et al.

A precedent for this notion comes from the observation that loss of both BAX and BAK, which renders cells completely apoptosis deficient, triggers increased autophagy and decreased mTOR signaling in response to stress signals, as a measure to maintain cell viability (39, 40). Loss of SIVA could similarly promote autophagy in the presence of a stress signal such as oncogenic KRAS. That SIVA loss could mimic BAX/BAK deficiency is consistent with the observation that BAX and BAK are required for SIVA to induce apoptosis (11). A role for SIVA at the mitochondria is further supported by the decreased mitochondrial function observed upon *SIVA* knockdown. Interestingly, mitochondrial respiration has been found to be required for mitochondrial apoptosis by allowing for efficient mitochondrial depolarization and release of proapoptotic factors (41, 42). Thus, diminished mitochondrial respiration may be a mechanism by which SIVA deficiency protects cells from apoptosis, in keeping with the important role for SIVA in apoptosis (11). Overall, elucidating the mechanisms through which SIVA deficiency inhibits mTOR signaling, dampens oxidative phosphorylation, and triggers autophagy will be an important future goal for understanding how SIVA promotes tumorigenesis.

In addition to defining a role for SIVA in efficient mTOR signaling, we also identified additional signaling pathways affected by SIVA status in our microarray experiments. One particularly interesting signaling pathway upregulated upon *SIVA* knockdown is the TBK1 pathway. TBK1 is an I $\kappa$ B kinase that promotes survival through the NF $\kappa$ B and AKT pathways and is required for KRAS-dependent NSCLC proliferation (26, 43). However, TBK1 has also been shown to inhibit mTOR activity and promote autophagy (44). Thus, although upregulation of TBK1 signaling could explain how *SIVA* deficiency inhibits mTOR activity and drives autophagy, the proproliferative activity attributed to activated TBK1 contrasts with the decreased proliferation observed upon SIVA inactivation, suggesting that TBK1 is not a primary SIVA mediator. Another intriguing signature associated with *SIVA* knockdown is activated HIPPO-YAP signaling. The YAP pathway controls organ size and tumorigenesis by promoting cell proliferation and inhibiting apoptosis (45). Moreover, YAP activates the P13K-mTOR pathway by inhibiting PTEN (37, 46). Therefore, it is possible that SIVA activates the mTOR pathway by activating the YAP pathway. Another signature identified upon *SIVA* knockdown is that of inhibition of BMI1, a component of the polycomb repressive complex, which promotes both cell self-renewal and tumorigenesis (47). Although loss of BMI1 results in decreased tumorigenic potential and decreased mitochondrial oxidative capacity, like SIVA loss, it is not known to promote other phenotypes associated with SIVA deficiency, such as inhibition of mTOR signaling (48). It will be of great interest in future studies to further evaluate the role of SIVA in these additional signaling pathways to better define the mechanisms by which SIVA promotes tumorigenesis.

Our finding that SIVA is necessary for efficient tumorigenesis in an autochthonous lung cancer model suggests the possibility of SIVA as a therapeutic target. Indeed, the protumorigenic role of SIVA is supported by a previous xenograft study in which *SIVA* knockdown in U2OS cells was found to inhibit tumor growth relative to control knockdown cells (14).

Furthermore, our finding that alternate cell types, including primary MEFs, are not adversely affected by SIVA loss suggests that SIVA inhibition could represent a useful strategy for cancer treatment. In future studies, it will also be interesting to further elaborate the role of SIVA *in vivo* using mouse models for other cancer types to determine whether SIVA generally plays an enabling role in tumorigenesis or if SIVA might play context-dependent roles in cancer development, sometimes suppressing tumor development. Regardless, the discovery of a role for SIVA in enhancing tumorigenesis unveils a potential new therapeutic target for cancer treatment.

## METHODS

**Generation of Siva Conditional Knockout Mice**

The *Siva* locus was isolated from a BAC clone, 122D14, obtained from the Sanger Institute (Cambridge, UK), using BspE1 and BstE11 restriction enzymes. The fragment including *Siva* was modified to incorporate a 5' LoxP site at the BspE1 site and a 3' Lox-PGK-Puro-Lox cassette at the BstE11 site and subcloned into the 184-DT-PL vector. The *Siva* targeting construct was introduced into J1 ES cells by electroporation. ES cells were cultured on irradiated MEF feeders in LIF-containing media (Millipore). Positive clones were identified by PCR and Southern blot analysis for both 5' and 3' targeting and used to generate chimeric mice at the Stanford transgenic research facility. Chimeras were bred to C57BL/6 females and progeny genotyped by Southern blot analysis or PCR as described below. Mice were further bred to CMV-Cre mice to excise the Puro cassette, resulting in a single LoxP site 3' of the *Siva* locus (*Siva*<sup>fl/fl</sup>). For analysis, *Siva* conditional mice were bred to *Kras*<sup>LSL-G12D/+</sup> mice. All animal work was done in accordance with the Stanford University (Stanford, CA) Administrative Panel on Laboratory Animal Care.

**Genotyping**

Genotyping was performed by PCR analysis of tail DNA. The primers used include a forward primer 5' for the LoxP site (F1: AGT ACC AGC ATT CCC TGG TG), a reverse primer 3' to the LoxP site (R1: GGA GTC AGA CCT CGT TAC GG), and a reverse primer 3' to the LoxPuroLox site (R2: CCA CAC AGG ACA TTC CAC AG).

**Lung Tumor Analysis**

For the tumor study, mice were intratracheally injected with  $4 \times 10^6$  plaque-forming units of Ad-Cre [University of Iowa Gene Transfer Vector Core (GTVC), Iowa City, IA], as described (18). Mice were sacrificed 18 weeks later for analysis of tumor number and burden. Lungs were paraformaldehyde-fixed, each lobe bisected or trisected, and paraffin-embedded. Histologic analysis was performed on hematoxylin and eosin-stained sections. Lung area and tumor area were quantified using ImageJ.

**Cell Culture**

LSZ2, LSZ4, A549, and *Trp53*-null NSCLC cells and MEFs were cultured in DMEM with 10% serum (3, 19). LSZ2 and LSZ4 cells were a gift from Alejandro Sweet-Cordero (Stanford School of Medicine, Stanford, CA). *Trp53* status was confirmed by Western blot analysis and target gene expression analyses, but cell lines were not otherwise authenticated. *Trp53*-null NSCLC cells were derived from *Kras*<sup>LAL2</sup>; *Trp53*-null mice as described previously (3). MEFs were derived from wild-type or *Siva*<sup>fl/fl</sup> E13.5 embryos, and genotypes were determined by PCR. Cells were last tested for *Mycoplasma* using Lonza MycoAlert Assay (LT07-118) at the time of revisions. Adenoviral infections were performed at a multiplicity of infection of approximately 100 using adenoviral Cre or empty (Ad-Cre or Ad-Emp; University of Iowa GTVC) for

24 hours. Cells were imaged using phase-contrast microscopy. For BrdUrd incorporation analysis, cells were incubated with 3 µg/mL BrdUrd for 4 hours before fixation of cells on coverslips using 4% paraformaldehyde. Cells were treated with 50 nmol/L rapamycin, 50 nmol/L Torin1, or 100 nmol/L chloroquine for 18 hours prior to the BrdUrd pulse. *Tsc2* was knocked down with Dharmacon smart pool siRNAs (cat. no. #L-047050-00) using Lipofectamine RNAiMax reagent (Life Technology), and cells were BrdUrd-pulsed 72 hours later. Immunofluorescence was performed as described with anti-BrdUrd antibody (1:50, 347580; BD Bioscience; ref. 5). Proliferation was monitored using a Sulforhodamine B assay as described (49) on trichloroacetic acid-fixed cells collected every 2 days over a 7-day period. For low plating assays, 150 cells were plated into 6-well dishes and collected 10 days later, and colonies were stained with crystal violet. For soft agar assays, 10<sup>5</sup> cells were cultured in 2.4% noble agar in DMEM with 10% serum for 2 or 3 weeks. Colonies were visualized after staining with 0.02% Giemsa and quantified using ImageJ on scanned images. For respiration rate analysis, 10<sup>4</sup> cells were plated in each well of a 96-well plate and analyzed for OCR and ECAR on an XF96 Extracellular Flux Analyzer (Seahorse Biosciences) upon treatment with oligomycin, FCCP, or antimycin. Rates were normalized to cell number.

### Western Blot Analysis

Cells were collected and lysed with RIPA buffer (1% NP40, 0.5% sodium deoxycholate, 0.1% SDS, Tris pH 8.0) with protease inhibitors (Complete; Roche) or SDS buffer (20% SDS, Tris pH 6.8) with protease and phosphatase inhibitors (Roche). Western blot analyses were probed with anti-p53 (1:500, CM5; Vector Labs), anti-LC3 (1:2,000, NB100-2220; Novus), anti-S6K (1:1,000, 9206; Cell Signaling Technology), anti-pS6K (1:1,000, 2708; Cell Signaling Technology), anti-4EBP1 (1:1,000, 9452; Cell Signaling Technology), anti-p4EBP1 (1:1,000, 9459; Cell Signaling Technology), anti-SIVA (1:500; J.V.N, see below), anti-pS6 (1:1,000, 4858; Cell Signaling Technology), anti-S6 (1:1,000, 2217; Cell Signaling Technology), anti-pRAPTOR (1:1,000, 2083; Cell Signaling Technology), anti-RAPTOR (1:1,000, 2280; Cell Signaling Technology), anti-pTSC2 (1:1,000, 3617; Cell Signaling Technology), anti-TSC2 (1:1,000, 3612; Cell Signaling Technology), anti-PARP (1:1,000, 9532; Cell Signaling Technology), or anti-Actin (1:30,000; Sigma; A2228). SIVA antibodies were generated by injecting rabbits with a recombinant mouse MBP-SIVA fusion protein and purified using recombinant GST-SIVA.

### qPCR

For qRT-PCR, NSCLC cells were cultured at subconfluence, RNA was isolated by TRIzol extraction and reverse transcribed using Moloney murine leukemia virus reverse transcriptase (Invitrogen) and random primers, and PCR was performed in triplicate using SYBR green (Qiagen, Bio-Rad) and specific primers for each gene (Supplementary Table S1) in a 7900HT Fast Real-Time PCR machine (Applied Biosystems). Results were computed relative to a standard curve made with cDNA pooled from all samples and normalized to  $\beta$ -Actin. For qPCR of mitochondrial DNA, NSCLC cells were cultured at subconfluence, cells were lysed in RIPA buffer with Proteinase K, and DNA was purified with phenol/chloroform extraction followed by ethanol precipitation. PCR was performed in triplicate using SYBR green (Qiagen, Bio-Rad) and mouse-specific primers for each mitochondrial gene. Results were computed relative to a standard curve made with DNA pooled from all samples and normalized to  $\beta$ -microglobulin.

### Microarray Analysis

Microarray analysis was performed on RNA isolated by TRIzol extraction from LSZ2 and LSZ4 cells transduced with two independent *Siva* shRNAs (sh*Siva1* and sh*Siva2*) or two control shRNAs (sh*GFP* and

sh*LacZ*). RNA was hybridized to Agilent Sureprint G3 Mouse GE 8 × 60 K microarrays (G4852A) by the Stanford Functional Genomics Facility (microarray data files were deposited at Gene Expression Omnibus: GSE66126) and data were normalized and analyzed using GeneSpring GX software (Agilent). GO annotation was performed using GeneSpring GX software, and GSEA was performed using GSEA software (50).

### Constructs

*Siva* knockdown was performed using two independent mouse shRNAs: LL37-GFP sh*Siva1* (GAGCGAAGATTGTTCCGTGAA; Broad Institute, Cambridge, MA) or pLKO TRC2 sh*Siva1* (GATTGTTCCGTG AACCAACC) and pLKO TRC2 sh*Siva2* (GGGCCTATAGAGATCACATAT); and one human shRNA: pLKO TRC2 sh*SIVA* (GCTACAGCTCAAGGCC GCGTC). *Trp53* knockdown was performed using an shRNA: LMN sh*Trp53* (CCCACTACAAGTACATGTGAA). pLKO TRC2 sh*GFP*, LMN sh*Luc*, or LL37-GFP sh*LacZ* were used as negative controls.

### Disclosure of Potential Conflicts of Interest

No potential conflicts of interest were disclosed.

### Authors' Contributions

**Conception and design:** J.L. Van Nostrand, S.B.R. Jacobs, L.D. Attardi  
**Development of methodology:** J.L. Van Nostrand  
**Acquisition of data (provided animals, acquired and managed patients, provided facilities, etc.):** J.L. Van Nostrand, A. Brisac  
**Analysis and interpretation of data (e.g., statistical analysis, biostatistics, computational analysis):** J.L. Van Nostrand, A. Brisac, S.S. Mello, R. Luong, L.D. Attardi  
**Writing, review, and/or revision of the manuscript:** J.L. Van Nostrand, A. Brisac, S.S. Mello, S.B.R. Jacobs, R. Luong, L.D. Attardi  
**Administrative, technical, or material support (i.e., reporting or organizing data, constructing databases):** J.L. Van Nostrand, R. Luong  
**Study supervision:** J.L. Van Nostrand, L.D. Attardi

### Acknowledgments

The authors thank R.J. Shaw for reading the article manuscript and S.E. Artandi for discussion. The authors also thank A. Sweet-Cordero for LSZ2 and LSZ4 cell lines; K.T. Biegling for the *Trp53*-null NSCLC cell line and *Trp53* shRNA construct; N. Bardeesy for pancreatic cancer cell lines; A. Flore for technical assistance with intratracheal injections for the lung tumor study; and L. Johnson and O. Foreman for assistance with histologic analysis of tumors. The authors thank the Stanford Functional Genomics Facility for assistance with microarray analysis and Agilent for providing microarrays, E. LaGory for assistance with the Seahorse Analyzer, and R. Shaw, A. Giaccia, and A. Brunet for mTOR pathway antibodies and reagents.

### Grant Support

This work was supported by funding from the National Science Foundation and NCI (grant number 1F31CA167917-01) to J.L. Van Nostrand and by funding from the American Cancer Society, Leukemia & Lymphoma Society, and NIH (RO1 CA140875) to L.D. Attardi.

The costs of publication of this article were defrayed in part by the payment of page charges. This article must therefore be hereby marked *advertisement* in accordance with 18 U.S.C. Section 1734 solely to indicate this fact.

Received August 19, 2014; revised March 18, 2015; accepted March 23, 2015; published OnlineFirst March 26, 2015.

### REFERENCES

1. Vousten KH, Prives C. Blinded by the light: the growing complexity of p53. *Cell* 2009;137:413–31.

## RESEARCH ARTICLE

## Van Nostrand et al.

2. Carvajal LA, Manfredi JJ. Another fork in the road—life or death decisions by the tumour suppressor p53. *EMBO Rep* 2013;14:414–21.
3. Kenzelmann Broz D, Mello SS, Bieging KT, Jiang D, Dusek RL, Brady CA, et al. Global genomic profiling reveals an extensive p53-regulated autophagy program contributing to key p53 responses. *Genes Dev* 2013;27:1016–31.
4. Bieging KT, Mello SS, Attardi LD. Unravelling mechanisms of p53-mediated tumour suppression. *Nat Rev Cancer* 2014;14:359–70.
5. Brady CA, Jiang D, Mello SS, Johnson TM, Jarvis LA, Kozak MM, et al. Distinct p53 transcriptional programs dictate acute DNA-damage responses and tumor suppression. *Cell* 2011;145:571–83.
6. Valente LJ, Gray Daniel HD, Michalak EM, Pinon-Hofbauer J, Egle A, Scott Clare L, et al. p53 efficiently suppresses tumor development in the complete absence of its cell-cycle inhibitory and proapoptotic effectors p21, Puma, and Noxa. *Cell Rep* 2013;3:1339–45.
7. Timofeev O, Schlereth K, Wanzel M, Braun A, Nieswandt B, Pagenstecher A, et al. p53 DNA binding cooperativity is essential for apoptosis and tumor suppression in vivo. *Cell Rep* 2013;3:1512–25.
8. Li T, Kon N, Jiang L, Tan M, Ludwig T, Zhao Y, et al. Tumor suppression in the absence of p53-mediated cell-cycle arrest, apoptosis, and senescence. *Cell* 2012;149:1269–83.
9. Prasad KV, Ao Z, Yoon Y, Wu MX, Rizk M, Jacquot S, et al. CD27, a member of the tumor necrosis factor receptor family, induces apoptosis and binds to Siva, a proapoptotic protein. *Proc Natl Acad Sci U S A* 1997;94:6346–51.
10. Spinicelli S, Nocentini G, Ronchetti S, Krausz LT, Bianchini R, Riccardi C. GITR interacts with the pro-apoptotic protein Siva and induces apoptosis. *Cell Death Differ* 2002;9:1382–4.
11. Jacobs S, Basak S, Murray JL, Pathak N, Attardi LD. Siva is an apoptosis-selective p53 target gene important for neuronal cell death. *Cell Death Differ* 2007;14:1374–85.
12. Fortin A, MacLaurin JG, Arbour N, Cregan SP, Kushwaha N, Callaghan SM, et al. The proapoptotic gene Siva is a direct transcriptional target for the tumor suppressors p53 and E2F1. *J Biol Chem* 2004;279:28706–14.
13. Py B, Slomiany C, Aubreger P, Petit PX, Benichou S. Siva-1 and an alternate splice form lacking the death domain, Siva-2, similarly induce apoptosis in T lymphocytes via a caspase-dependent mitochondrial pathway. *J Immunol* 2004;172:4008–17.
14. Du W, Jiang P, Li N, Mei Y, Wang X, Wen L, et al. Suppression of p53 activity by Siva1. *Cell Death Differ* 2009;16:1493–504.
15. Wang X, Zha M, Zhao X, Jiang P, Du W, Tam A, et al. Siva1 inhibits p53 function by acting as an ARF E3 ubiquitin ligase. *Nat Commun* 2013;4:1551.
16. Hildebrandt T, Preiherr J, Tarbe N, Klostermann S, Van Muijen GN, Weidle UH. Identification of THW, a putative new tumor suppressor gene. *Anticancer Res* 2000;20:2801–9.
17. Jackson EL, Olive KP, Tuveson DA, Bronson R, Crowley D, Brown M, et al. The differential effects of mutant p53 alleles on advanced murine lung cancer. *Cancer Res* 2005;65:10280–8.
18. Dupage M, Dooley AL, Jacks T. Conditional mouse lung cancer models using adenoviral or lentiviral delivery of Cre recombinase. *Nat Protoc* 2009;4:1064–72.
19. Vicent S, Sayles LC, Vaka D, Khatri P, Gevaert O, Chen R, et al. Cross-species functional analysis of cancer-associated fibroblasts identifies a critical role for Clcf1 and Il-6 in non-small cell lung cancer in vivo. *Cancer Res* 2012;72:5744–56.
20. Györffy B, Lánczyk A, Szálássai Z. Implementing an online tool for genome-wide validation of survival-associated biomarkers in ovarian cancer using microarray data from 1287 patients. *Endocr Relat Cancer* 2012;19:197–208.
21. Györffy B, Surowiak P, Budczies J, Lánczyk A. Online survival analysis software to assess the prognostic value of biomarkers using transcriptomic data in non-small-cell lung cancer. *PLoS ONE* 2013;8:E82241.
22. Wu J, Powell F, Larsen NA, Lai Z, Byth KF, Read J, et al. Mechanism and *in vitro* pharmacology of TAK1 inhibition by (5z)-7-oxozeanol. *ACS Chem Biol* 2012;8:643–50.
23. Resch U, Schichl YM, Winsauer G, Gudi R, Prasad K, De Martin R. Siva1 is a xiap-interacting protein that balances NF{Kappa}B and JNK signalling to promote apoptosis. *J Cell Sci* 2009;122:2651–61.
24. Fimia GM, Stoykova A, Romagnoli A, Giunta L, Di Bartolomeo S, Nardacci R, et al. AMBRA1 regulates autophagy and development of the nervous system. *Nature* 2007;447:1121–5.
25. Liang C, Feng P, Ku B, Dotan I, Canaani D, Oh B-H, et al. Autophagic and tumour suppressor activity of a novel Beclin1-binding protein UVrag. *Nat Cell Biol* 2006;8:688–98.
26. Pomerantz JL, Baltimore D. NF-κB activation by a signaling complex containing TRAF2, TANK and TBK1, a novel IKK-related kinase. *EMBO J* 1999;18:6694–704.
27. Huang K, Fingar DC. Growing knowledge of the mTOR signaling network. *Semin Cell Dev Biol* 2014;36:79–90.
28. Liang MC, Ma J, Chen L, Kozlowski P, Qin W, Li D, et al. TSC1 loss synergizes with KRAS activation in lung cancer development in the mouse and confers rapamycin sensitivity. *Oncogene* 2010;29:1588–97.
29. Menon S, Yecies JL, Zhang HH, Howell JJ, Nicholatos J, Harputlugil E, et al. Chronic activation of mTOR complex 1 is sufficient to cause hepatocellular carcinoma in mice. *Sci Signal* 2012;5:ra24.
30. Rao S, Tortola L, Perlot T, Wirnsberger G, Novatchkova M, Nitsch R, et al. A dual role for autophagy in a murine model of lung cancer. *Nat Commun* 2014;5:3056.
31. Pierce AM, Schneider-Broussard R, Gimenez-Conti IB, Russell JL, Conti CJ, Johnson DG. E2F1 has both oncogenic and tumor-suppressive properties in a transgenic model. *Mol Cell Biol* 1999;19:6408–14.
32. Cheung EC, Athineos D, Lee P, Ridgway RA, Lambie W, Nixon C, et al. TIGAR is required for efficient intestinal regeneration and tumorigenesis. *Dev Cell* 2013;25:463–77.
33. Lee P, Vousden K, Cheung E. TIGAR, TIGAR, burning bright. *Cancer Metab* 2014;2:1.
34. Morita M, Gravel S-P, Chénard V, Sikström K, Zheng L, Alain T, et al. mTORC1 controls mitochondrial activity and biogenesis through 4E-BP-dependent translational regulation. *Cell Metab* 2013;18:698–711.
35. Schieke SM, Phillips D, Mccoy JP, Aponte AM, Shen R-F, Balaban RS, et al. The mammalian target of rapamycin (mTOR) pathway regulates mitochondrial oxygen consumption and oxidative capacity. *J Biol Chem* 2006;281:27643–52.
36. Egan D, Kim J, Shaw RJ, Guan K-L. The autophagy initiating kinase ULK1 is regulated via opposing phosphorylation by AMPK and mTOR. *Autophagy* 2011;7:643–4.
37. Shimobayashi M, Hall MN. Making new contacts: the mTOR network in metabolism and signalling crosstalk. *Nat Rev Mol Cell Biol* 2014;15:155–62.
38. Dong L-X, Sun L-L, Zhang X, Pan L, Lian L-J, Chen Z, et al. Negative regulation of mTOR activity by LKB1-AMPK signaling in non-small cell lung cancer cells. *Acta Pharmacol Sin* 2013;34:314–8.
39. Lum JJ, Bauer DE, Kong M, Harris MH, Li C, Lindsten T, et al. Growth factor regulation of autophagy and cell survival in the absence of apoptosis. *Cell* 2005;120:237–48.
40. Kim KW, Mutter RW, Cao C, Albert JM, Freeman M, Hallahan DE, et al. Autophagy for cancer therapy through inhibition of pro-apoptotic proteins and mammalian target of rapamycin signaling. *J Biol Chem* 2006;281:36883–90.
41. Kwong JQ, Henning MS, Starkov AA, Manfredi G. The mitochondrial respiratory chain is a modulator of apoptosis. *J Cell Biol* 2007;179:1163–77.
42. Ballot C, Kluzo J, Lancel S, Martoriati A, Hassoun S, Mortier L, et al. Inhibition of mitochondrial respiration mediates apoptosis induced by the anti-tumoral alkaloid lamellarin D. *Apoptosis* 2010;15:769–81.
43. Newman AC, Scholefield CL, Kemp AJ, Newman M, Mciver EG, Kamal A, et al. TBK1 kinase addiction in lung cancer cells is mediated via autophagy of TAX1BP1/NDP52 and non-canonical NF-κB signalling. *PLoS ONE* 2012;7:E50672.
44. Kim JK, Jung Y, Wang J, Joseph J, Mishra A, Hill EE, et al. TBK1 regulates prostate cancer dormancy through mTOR inhibition. *Neoplasia* 2013;15:1064–74.

45. Zhao B, Li L, Lei Q, Guan K-L. The HIPPO-YAP pathway in organ size control and tumorigenesis: an updated version. *Genes Dev* 2010;24:862–74.
46. Tumaneng K, Schlegelmilch K, Russell RC, Yimlamai D, Basnet H, Mahadevan N, et al. YAP mediates crosstalk between the Hippo and PI(3)K-TOR pathways by suppressing pTEN via miR-29. *Nat Cell Biol* 2012;14:1322–9.
47. Dovey JS, Zacharek SJ, Kim CF, Lees JA. BMI1 is critical for lung tumorigenesis and bronchioalveolar stem cell expansion. *Proc Natl Acad Sci U S A* 2008;105:11857–62.
48. Liu J, Cao L, Chen J, Song S, Lee IH, Quijano C, et al. BMI1 regulates mitochondrial function and the DNA damage response pathway. *Nature* 2009;459:387–92.
49. Voigt W. Sulforhodamine B assay and chemosensitivity. In: Blumenthal R, editor. *Cancer Chemotherapy: Principles and Practice*. Totowa, NJ: Humana Press; 2005. p. 39–48.
50. Subramanian A, Tamayo P, Mootha VK, Mukherjee S, Ebert BL, Gillette MA, et al. Gene set enrichment analysis: a knowledge-based approach for interpreting genome-wide expression profiles. *Proc Natl Acad Sci U S A* 2005;102:15545–50.

# CANCER DISCOVERY

## The p53 Target Gene SIVA Enables Non–Small Cell Lung Cancer Development

Jeanine L. Van Nostrand, Alice Brisac, Stephano S. Mello, et al.

*Cancer Discovery* 2015;5:622-635. Published OnlineFirst March 26, 2015.

**Updated version** Access the most recent version of this article at:  
[doi:10.1158/2159-8290.CD-14-0921](https://doi.org/10.1158/2159-8290.CD-14-0921)

**Supplementary Material** Access the most recent supplemental material at:  
<http://cancerdiscovery.aacrjournals.org/content/suppl/2015/03/26/2159-8290.CD-14-0921.DC1>

**Cited articles** This article cites 49 articles, 18 of which you can access for free at:  
<http://cancerdiscovery.aacrjournals.org/content/5/6/622.full#ref-list-1>

**E-mail alerts** [Sign up to receive free email-alerts](#) related to this article or journal.

**Reprints and Subscriptions** To order reprints of this article or to subscribe to the journal, contact the AACR Publications Department at  
[pubs@aacr.org](mailto:pubs@aacr.org).

**Permissions** To request permission to re-use all or part of this article, contact the AACR Publications Department at  
[permissions@aacr.org](mailto:permissions@aacr.org).